


Multi-Omics Analysis Revealed That TAOK1 Can Be Used as a Prognostic Marker and Target in a Variety of Tumors, Especially in Cervical Cancer

Li Ning^{1,2}, Xiu Li^{1,2}, Yating Xu^{1,2}, Yu Si^{1,2}, Hongting Zhao², Qingling Ren^{1,2} 

¹The Affiliated Hospital of Nanjing University of Chinese Medicine, Nanjing, People's Republic of China; ²The Chinese Clinical Medicine Innovation Center of Obstetrics, Gynecology, and Reproduction in Jiangsu Province, Nanjing, Jiangsu, People's Republic of China

Correspondence: Qingling Ren, The Affiliated Hospital of Nanjing University of Chinese Medicine, Nanjing, People's Republic of China, Email yfy0047@njucm.edu.cn

Background: Thousand and One Kinase 1 (TAOK1), a member of the MAPK kinase family, plays a crucial role in processes like microtubule dynamics, DNA damage response, and neurodevelopment. While TAOK1 is linked to tumorigenesis, its oncogenic role across cancers remains unclear. This study aims to explore the relationship between TAOK1 expression, prognosis, and immune function in various cancers.

Methods: We analyzed TAOK1 expression in multiple cancers using TCGA, GEO, CCLE, and other bioinformatics databases. The correlation between TAOK1 expression and immune cell infiltration was assessed with the ESTIMATE algorithm. We also examined associations with tumor stemness, DNA methylation, gene copy number alterations, and drug sensitivity. The oncogenic role of TAOK1 was further evaluated in vitro with SiHa and A2780 cells and in vivo with TAOK1 overexpression in SiHa cells.

Results: TAOK1 is a key prognostic biomarker in various cancers and its high expression is associated with poor prognosis. It showed a significant negative correlation with immune cell infiltration and immune checkpoints. GSEA identified its involvement in key tumour pathways, highlighting the therapeutic potential of inhibiting the TAOK1 gene. The high expression of TAOK1 is associated with DNA methylation and gene copy number variation, and in addition its upstream regulator, EP300, is closely associated with TAOK1 expression. In vitro cellular experiments demonstrated that inhibition of TAOK1 reduced the proliferation of SiHa and A2780 cells, whereas overexpression of TAOK1 in SiHa cells promoted growth. These findings were further validated in vivo by nude mouse tumorigenicity assay and human tissue immunohistochemistry.

Conclusion: TAOK1 serves as a promising prognostic biomarker and potential therapeutic target, especially for cervical cancer. These results support its clinical potential in cancer prognosis and treatment strategies.

Keywords: TAOK1, prognosis, pan-cancer analysis, methylation, immunoinfiltration analysis

Introduction

Malignant tumors persist as a paramount threat to human life despite significant advancements in tumor prevention screening,¹ multi-disciplinary treatment approaches, precision medicine, and novel drug development.² Consequently, there remains an imperative to extend patient survival and refine treatment strategies. In this context, gene therapy emerges as a promising frontier in cancer treatment, the development of new biomarkers is crucial for the treatment of tumors.^{3,4}

The STE20 protein (Sterile 20) kinase family plays a pivotal role in cancer cell proliferation and transformation.⁵ While STE20 kinase inhibitors have been developed and employed in potential cancer therapies,^{6,7} further evidence is required to validate their efficacy. The STE20 family contains 30 serine-threonine kinases, which are divided into 10 subfamilies, among which the TAOK subfamily (thousand and one kinases) mainly consists of TAOK1, TAOK2 and TAOK3.⁸ Inhibition of TAOK has been demonstrated to augment centrosome deaggregation and mitosis in cancer cells.⁹ Noteworthy research has elucidated TAOK1's capacity to activate MAPK signaling cascades, thus influencing cellular

architecture.¹⁰ Extensive investigations have revealed dysregulation of TAOK1 across various tumor types, including breast cancer,¹¹ esophageal squamous cell carcinoma,¹² non-small cell lung cancer,¹³ colon cancer,¹⁴ and ovarian cancer,¹⁵ implicating its pivotal role in tumor regulation. Furthermore, Mikhail Liskovych suggests TAOK1's involvement in chromosomal instability (CIN), underscoring its relevance in addressing CIN-related cancers.¹⁶

In most of the studies, TAOK1 showed significant tumor-promoting effects, but the exact mechanism of action involved is not clear. To comprehensively elucidate the function and significance of TAOK1 in different tumor types, we employed a series of analyses. Comprehensive analyses, including differential analysis, methylation analysis, and immune infiltration analysis, collectively highlighted the critical role of TAOK1. In addition, *in vivo* and *in vitro* experiments provided additional support for the regulatory mechanisms of TAOK1, thus providing valuable insights for future studies focusing on TAOK1.

Material and Methods

Patient Data and Preprocessing in Different Tumors

The mRNA expression data for TAOK1 were primarily sourced from the UCSC Xena Browser, which houses 19,131 samples (<https://xena.ucsc.edu/>). Diverse datasets were extracted from this resource, encompassing gene expression (selected TPMs), mutation data, clinical information, survival outcomes, DNA methylation profiles, and stemness scores derived from mRNA expression and DNA methylation data. The TCGA database includes 33 different tumor tissues and clinical samples, and the GTEx database includes 31 different tumor normal samples. It is imperative to note that the UCSC team integrated data from these two distinct databases and performed batch effect removal.

Additionally, to elucidate the expression levels of TAOK1 in more detail, we obtained datasets for four tumor types from the GEO (Gene Expression Omnibus) database. These datasets include the gastric cancer database GSE64951 (platform: GPL570-55999),¹⁷ the liver cancer database GSE174570 (platform: GPL13667-1557),¹⁸ the ovarian cancer database GSE26712 (platform: GPL96-57554),¹⁹ and the lung adenocarcinoma database GSE43767 (platform: GPL6480-9577).²⁰ Expression profiles and copy number alterations were log-normalized using GISTIC2.0, with TPM values adjusted to 0.001. Additionally, protein expression data for various tumor types were retrieved from the Clinical Proteomic Tumor Analysis Consortium (CPTAC) website. Cell line data were sourced from the Cancer Cell Line Encyclopedia (CCLE) website. Information on immune cell infiltration in different tumor types was collected from the Tumor Immunity Estimation Resource (TIMER) 2.0 website. Transcription factor analysis was conducted using three websites: hTFTarget, ENCODE, and Cistrome DB. The workflow diagram used in this study is shown in Figure 1.

Survival Analysis of TAOK1

We evaluated the relationship between TAOK1 expression levels and multiple prognostic factors in cancer patients, such as overall survival (OS), disease-specific survival (DSS), progression-free interval (DFI), and progression-free survival (PFS), by analyzing survival data from TCGA. Statistical analysis, including Cox regression and Kaplan-Meier curve analysis, was performed using the “survival” and “survminer” R packages and “ggplot2” for creating forest plots based on the median levels observed in different tumor types.

Drug Sensitivity Analysis of TAOK1

We conducted a study using the GDSC V2 database to examine the correlation between TAOK1 and the efficacy of 198 drugs. The association between TAOK1 and drug sensitivity was evaluated using the oncopredict tool. Additionally, we examined the correlation between antitumor drug sensitivity and TAOK1 expression using the Cellminer database. This combined analysis enabled us to explore the potential link between TAOK1 expression and sensitivity to various therapeutic drugs.

Correlation Analysis of TAOK1 With Immune Microenvironment, Immune Checkpoints, Genomic Mutation Profiles and Tumour Stemness Score

In order to gain a comprehensive understanding of TAOK1's involvement, we conducted a joint analysis encompassing various aspects of the immune microenvironment and tumor characteristics. Initially, We performed an analysis using the

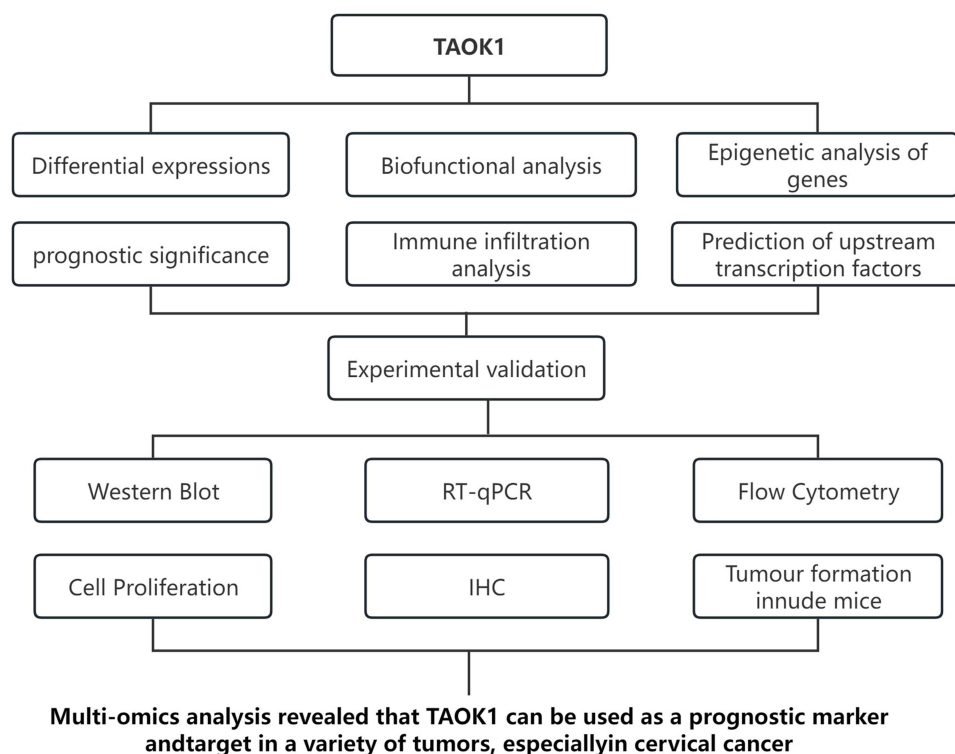


Figure 1 Flowchart of pan-cancer analysis of TAOK1.

R package “estimate” to investigate the association between intratumoral stromal and immune cell populations and TAOK1 expression. Additionally, the TIMER2 tool was used to examine the association between TAOK1 and different immune-infiltrating cell populations.

Moreover, we examined 11 immune checkpoint genes identified through literature searches, along with their expression profiles extracted from the TCGA database. These were subjected to correlation analysis with TAOK1 expression, aiming to uncover potential associations between TAOK1 and immune checkpoint regulation. We utilized the “Fmsb” R package to create radar plots illustrating Tumor Mutation Burden (TMB) and Microsatellite Instability (MSI), facilitating comprehensive analysis.

Furthermore, RNA expression and DNA methylation data from pan-cancer cohorts were extracted for correlation analysis of RNA-seq and DNA methylation signatures, employing the “corrplot” and “limma” R packages. The Spearman correlation method was consistently applied across all correlation analyses, ensuring robust statistical evaluation of TAOK1’s relationships with the immune microenvironment, genomic characteristics, and tumor stemness score.

TAOK1 Related Biological Processes and Gene Correlation Analysis

To delve into the functional implications of TAOK1 across diverse tumor types, we conducted Gene Set Enrichment Analysis (GSEA) utilizing data from TCGA. Through meticulous curation, genes exhibiting significant correlation with TAOK1 were pinpointed for enrichment analysis. Furthermore, genes participating in pivotal cellular processes such as cuproptosis, ferroptosis,²¹ and cell cycle regulation underwent correlation analysis.

The exploration of signaling pathways linked with TAOK1 was facilitated by the “clusterProfiler” package in R. In this study, we mainly exploited carefully curated genetic datasets, specifically “c2.cp.kegg.v7.5.1.entrez.gmt” and “c5.go.bp.v2023.2.Hs.entrez.gmt”, conduct a thorough GSEA analysis. This approach allowed us to unveil the intricate interplay between TAOK1 and various biological processes, shedding light on its potential roles in tumor progression and regulation.

Prediction of the Upstream Transcription Factors of the TAOK1 Gene

To uncover the upstream transcription factors governing TAOK1 expression, we explored three primary databases: hTFTarget, ENCODE, and Cistrome. This comprehensive analysis aimed to elucidate the regulatory network orchestrating TAOK1 expression. Additionally, predictive analytics were conducted by integrating data from ovarian cancer (OV) and cervical cancer (CESC) datasets sourced from TCGA, combined with the aforementioned online resources.

After collecting the data, the R package “ggplot2” was used for correlation analysis. This crucial step facilitated a thorough examination of the relationships between TAOK1 and its potential transcriptional regulators, thus shedding light on the underlying regulatory mechanisms governing TAOK1 expression within the context of ovarian and cervical cancers.

Cell Culture

The human cervical squamous carcinoma cell line SiHa, the human ovarian cancer cell line A2780, and the human renal epithelial cell line 293T were obtained from ATCC. SiHa and HEK 293T cells were cultured in Dulbecco's Modified Eagle Medium (DMEM; KGL1201-500; KeyGEN BioTECH, China) as per the manufacturer's instructions, while A2780 cells were cultured in RPMI-1640 medium (KGL1503-500; KeyGEN BioTECH, China). Both media were supplemented with 10% fetal bovine serum (FBS; C04001-500; Biological Industries, USA) and Penicillin / Streptomycin / Amphotericin B (P7630; Beijing Solebo Technology Co., Ltd.). The cells were maintained under standard conditions at 37°C in a humidified incubator with 5% CO₂. Routine mycoplasma contamination testing was carried out to ensure the integrity and quality of the cell cultures.

TAOK1 Small Interference and Transfection

Three unique small interfering RNA sequences for TAOK1, labeled Si-1, Si-2, and Si-3, were synthesized by Starfish Biologics and included in [Supplementary Table 2](#). Additionally, a negative control siRNA (NC) is provided. After synthesis, cells were seeded onto six-well plates to reach an approximate confluence of 40% and subsequently incubated for 24 hours.

Transfection was carried out using the siTran 2.0™ Transfection Kit (TT320002, Origene, China), strictly following the manufacturer's protocol. Post-transfection, the medium was replaced within 8–12 hours. The effect of transfection was then evaluated by Western blot analysis and reverse transcription real-time quantitative PCR to ensure the success of subsequent experiments.

Construction of Stable TAOK1 Overexpression Cell Lines

To establish TAOK1 overexpression cell lines, the plasmid containing TAOK1 gene was co-transfected with lentiviral packaging plasmid pCMV-dR8.9 and envelope plasmid pCMV-VSV-G to generate TAOK1 overexpression lentivirus in 293T cells. The overexpression plasmid and lentiviral packaging plasmid of TAOK1 were purchased from Shanghai Sangong Biotechnology Company Limited. The lentiviral solution was then added to SiHa cells and incubated for 6 h. Subsequently, the solution was changed to continue the incubation, and after 72 h, the cell morphology was observed, and the fluorescence was examined using an inverted fluorescence microscope (Ts2; Nikon) to assess the transfection efficiency. Subsequently, RT-qPCR was performed to verify the mRNA expression of TAOK1. Meanwhile, G418 (T6512; TargetMol) resistance was used to confirm stable overexpression of TAOK1. G418 was selected starting at 24 h post-infection and continuing for 14–17 days to identify stable TAOK1-OE of the SiHa for the selection of stable clones.

Protein Extraction and Western Blot

SiHa and A2780 cells were seeded into six-well plates respectively, and simultaneously transfected with three specific siRNA sequences targeting TAOK1 and non-targeting NC sequences. Cells underwent PBS rinses and trypsinization for 3–4 min. Subsequently, cells were lysed using RIPA lysis buffer containing protease and phosphatase inhibitors at a ratio of 48:1:1. The cells were lysed on ice for 10 minutes, followed by sonication for 1–2 cycles using a cell sonicator. After

lysis, centrifuge at 4°C for 15 min to remove cell debris. The total protein content in the lysates was quantified using the BCA Protein Quantification Kit (20201ES86; Yeasen). For Western blotting, 10 µg of protein was uniformly loaded onto a 10% SDS-PAGE gel and separated electrophoretically. Proteins separated by electrophoresis were then transferred to polyvinylidene fluoride (PVDF) membranes (IPVH00010; Merck Millipore). Incubate the membrane in Rapid Blocking Buffer (Cat. No. P30500; NCM) for 20 minutes at room temperature to minimize nonspecific binding. After blocking, the membrane was incubated with primary antibodies, including anti-TAOK1 (Cat. No. 26250-1-AP; Proteintech) and anti-β-actin (A17910; ABclonal), overnight at 4°C. The following day, wash three times with tris-buffered saline with Tween20 (TBST) to remove any unbound antibody. Anti-rabbit secondary antibody (ZB-2306; ZSGB-Bio) was incubated for 1 h at room temperature. After the exposure process is complete, use ImageJ software to visualize and quantify the protein bands present on the membrane, with β-actin as an internal control.

Cell Proliferation and Cell Cycle Detection

Cell proliferation was assessed using the CCK-8 assay kit (Cat. No. C0005; TargetMol). Cells were seeded in 96-well plates, and after adhesion, their absorbance was measured at 24, 48, and 72 hours. To evaluate cell proliferation, 10 µL of CCK-8 reagent was added to each well, and the cells were incubated at 37°C with 5% CO₂ for 1 hour. The absorbance at 450 nm was then measured using a microplate reader to determine cell viability.

Additionally, the cell cycle distribution of the two cell types was analyzed using propidium iodide (PI) dye. The transfected cells were seeded into a six-well plate and cultured. Cells were collected, rinsed with PBS, and then fixed in pre-chilled alcohol for 8 hours. Following this, cells were centrifuged, rehydrated, and stained with RNase A and propidium iodide (PI) (G1021; Servicebio). Following a 20-minute incubation in darkness at ambient temperature, cell cycle analysis was performed utilizing FACS Calibur flow cytometry (BD; USA).

The RNA Extraction and RT- qPCR

Total RNA was extracted using RNAeasy™ kit (R0027; Beyotime Biotechnology) following the manufacturer's protocol. The extracted total RNA was then reverse transcribed into complementary DNA (cDNA) using SuperMix (R323-01; Vazyme). After cDNA synthesis, quantitative polymerase chain reaction (qPCR) was conducted on Quantstudio 5 instrumentation using SYBR Green PCR Master Mix (Q311-02; Vazyme), with GAPDH serving as the internal reference gene for normalization. Primer sequences targeting the ten transcription factors and TAOK1 are provided in [Supplementary Table 1](#).

In vivo Animal Study

Thymus-free female BALB/c nude mice (4–6 weeks old) were purchased from Nanjing Carles Biotechnology Co., Ltd. and maintained under controlled conditions in the Central Laboratory of Jiangsu Provincial Hospital of Traditional Chinese Medicine. The mice were housed at a constant temperature of 23–25°C with a controlled light/dark cycle. A total of 1×10^8 control or TAOK1-overexpressing (TAOK1-OE) cells were resuspended in 150 µL of PBS buffer and subcutaneously injected into the right flank of the female nude mice. Injections were performed within 30 minutes of cell preparation. Mice were monitored until visible tumor formation occurred. All animals were euthanized on the 14th day post-injection, and the tumors were excised and photographed. The study was conducted in strict accordance with the guidelines in the National Institutes of Health Guide for the Care and Use of Laboratory Animals and was approved by the Ethics Committee of the Affiliated Hospital of Nanjing University of Traditional Chinese Medicine.

Immunohistochemical Analysis

A total of 16 tissue samples, including 8 cervical cancer tissues and 8 adjacent non-cancerous tissues, were collected from patients at Jiangsu Provincial Hospital of Traditional Chinese Medicine. The study was approved by the Ethics Committee of the Affiliated Hospital of Nanjing University of Chinese Medicine (Approval No. 2021NL-025-03). Written informed consent was obtained from all participants, or their legal guardians, prior to tissue collection, ensuring they fully understood the study's purpose, procedures, and potential risks. Tissues were fixed in paraformaldehyde, and the embedded wax blocks were sectioned into thin slices. The sections were then dewaxed and rehydrated using standard

protocols for antigen retrieval. Endogenous peroxidase activity was blocked by incubation with 3% hydrogen peroxide at room temperature, protected from light, for 30 minutes. Following three washes with PBS, the tissue sections were incubated with TAOK1 primary antibody overnight at 4°C. The next day, the sections were washed with PBS, and the appropriate secondary antibody was applied for 1 hour at room temperature. After PBS washes, color development, counterstaining, dehydration, and transparency steps were carried out. The slides were sealed and air-dried, then scanned using a tissue microarray scanner. The expression level of TAOK1 was quantified using Image J software.

Statistical Analysis

Statistical analyses were conducted using R (version 4.3.3). Spearman correlation coefficient was applied to assess the relationship between TAOK1 and various parameters, including immune cell infiltration, immune regulatory factors, methylation status, copy number variation, and tumor mutation burden. Results from *in vivo* and *in vitro* experiments were presented as means \pm standard deviations and analyzed using GraphPad Prism 9.5.1. Group comparisons were performed using either a *t*-test or one-way analysis of variance (ANOVA), as appropriate. Statistical significance was indicated as follows: **p* < 0.05, ***p* < 0.01, and ****p* < 0.001.

Result

Multi-Level Analysis of TAOK1 Expression in Different Tumors

To investigate TAOK1 expression across various cancer types, we conducted separate analyses of mRNA and protein levels. Analysis of variance based only on the TCGA database showed that TAOK1 expression was elevated in six cancer types with $\log_2 > 0.5$ and in two cancer types with $\log_2 > 1$. In contrast, TAOK1 mRNA was decreased in five tumor types ([Supplementary Table 3](#)). Subsequent analysis combining GTEx and TCGA samples unveiled a significant increase in TAOK1 expression in 12 cancer types, with $\log_2 > 1$ in 5 cancer types and $\log_2 > 0.5$ in most cancer types, including glioma (LGG), glioblastoma (GBM), pancreatic adenocarcinoma (PAAD), esophageal Cancer (ESCA), and stomach Adenocarcinoma (STAD); whereas expression levels were diminished in 5 cancer types, such as thymoma (THYM), renal papillary cell carcinoma (KIRP), acute myeloid Leukemia (LAML), and cholangiocarcinoma (CHOL). Furthermore, TAOK1 expression was reduced in 11 other cancer types, including endometrial Carcinoma (UCEC), and adrenocortical Carcinoma (ACC) ([Supplementary Table 4](#) and [Figure 2A](#)). Additionally, a paired *t*-test revealed a significant upregulation of expression in 10 tumor types compared to paired adjacent normal tissues ([Supplementary Table 5](#)), including breast cancer (BRCA), cholangiocarcinoma (CHOL), colorectal cancer (COAD), head and neck squamous cell carcinoma (HNSC), Kidney Renal Clear Cell Carcinoma (KIRC) and lung squamous cell carcinoma (LUSC) where the *p*-value was < 0.001 ([Supplement Figure 1](#)). To validate the expression of TAOK1 in different cancer types, we examined six TAOK1 transcripts, including two noncoding transcripts and four coding transcripts. Our analysis showed that the expression of non-coding transcripts significantly decreased, while the expression of coding transcripts increased significantly in various cancer types ([Supplement Figure 2A](#)). At the protein level, TAOK1 expression was predominantly increased in most tumour types, including renal cell carcinoma (CCRCC), hepatocellular carcinoma (HCC), and ovarian carcinoma (OV), in 13 datasets of 13 cancers in the CPTAC database ([Figure 2B](#)). We also analyzed the expression of TAOK1 in the four GEO datasets and showed a significant increase in its expression in the lung adenocarcinoma tumor dataset GSE43767 ([Figure 2C](#)), the esophageal squamous carcinoma dataset GSE6495 ([Figure 2D](#)), and the hepatocellular carcinoma dataset GSE174570 ([Figure 2E](#)) as well as increased expression in the ovarian cancer dataset GSE26712 ([Figure 2F](#)). The results of the study indicated that TAOK was not a significant factor. The results suggest that TAOK1 has an oncogenic role in a variety of cancer types.

Correlation of TAOK1 Prognosis in Different Cancer Types

To comprehensively investigate the prognostic significance of TAOK1 across various cancer types, we conducted an extensive analysis utilizing data from 33 cancers available in the TCGA database. We evaluated the association between TAOK1 expression and patients' overall survival (OS), disease-specific survival (DSS), disease-free interval (DFI), and progression-free interval (PFI) ([Figure 3A](#)).

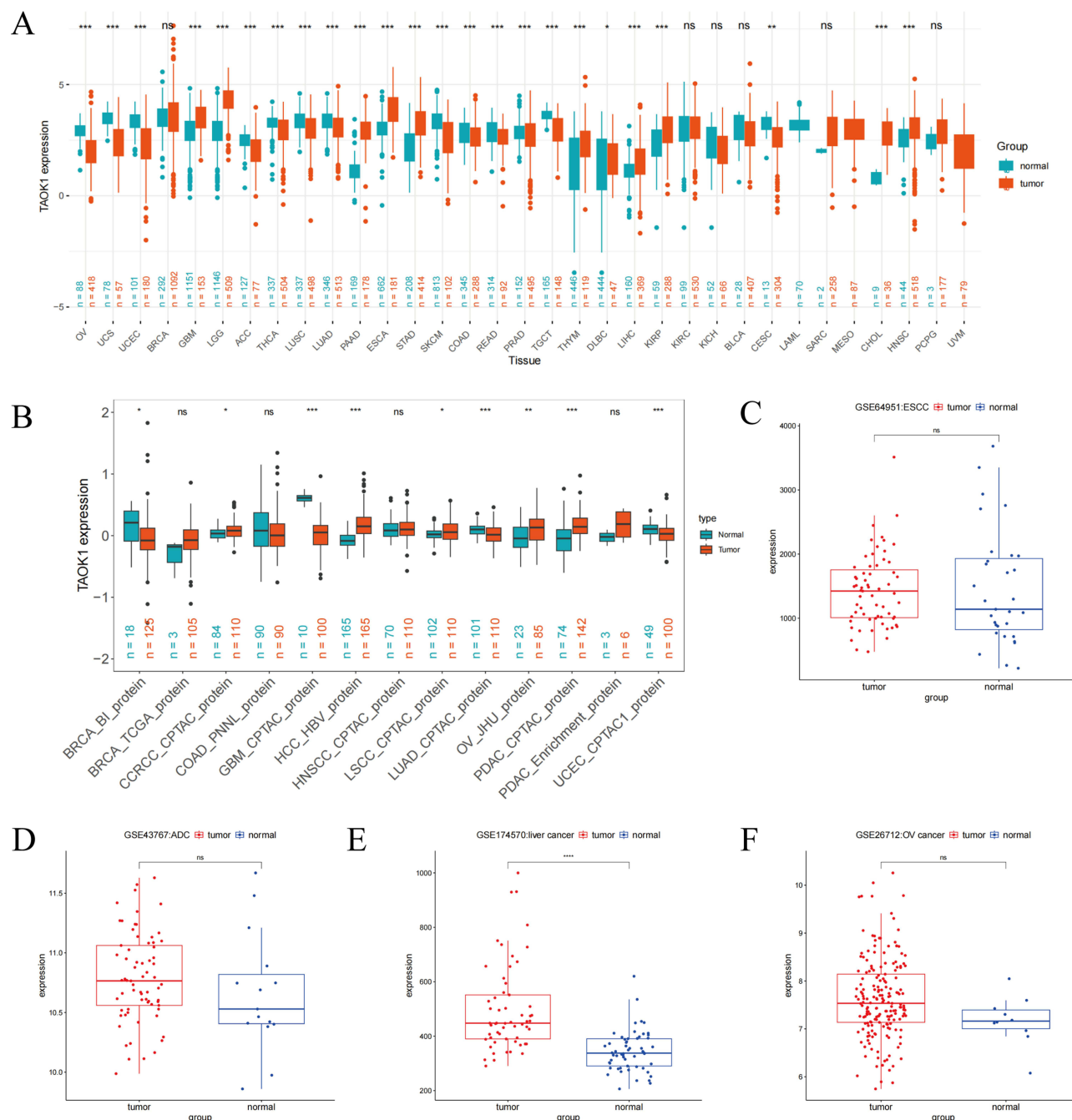


Figure 2 Examination of variations in mRNA and protein expression levels of TAOK1 among diverse tumor types. **(A)** The analysis of TAOK1 mRNA expression levels across 33 tumor types using data from The Cancer Genome Atlas (TCGA) combined with the Genotype-Tissue Expression (GTEx) database. Normal tissue samples are denoted in blue, while tumor samples are indicated in red. ns, not significant. **(B)** Protein expression levels of TAOK1 were analyzed across 14 types of tumors utilizing data from the Clinical Proteomic Tumor Analysis Consortium (CPTAC) database. **(C)** TAOK1 expression in four Gene Expression Omnibus (GEO) datasets was assessed: GSE43767, pertaining to adenocarcinoma (ADC); **(D)** GSE64951, focusing on esophageal squamous cell carcinoma (ESCC); **(E)** GSE174570, concerning liver cancer; and **(F)** GSE26712, related to ovarian cancer. Statistical significance is denoted as ns, not significant; * $P < 0.05$; ** $P < 0.01$; *** $P < 0.001$; **** $P < 0.0001$.

The results of OS and DSS analyses suggest that TAOK1 may be a high-risk factor for ACC and KICH, while it may play a preventive role in KIRC. Consistent trends were observed in analyses of DFI and PFI, reaffirming the findings from OS and DSS assessments. Moreover, Kaplan-Meier analysis demonstrated a significant correlation between high TAOK1 expression and unfavorable progression-free interval outcomes in various tumor types, such as ACC, BLCA, CESC, and UVM. Conversely, in KIRC, higher TAOK1 expression was linked to improved progression-free interval

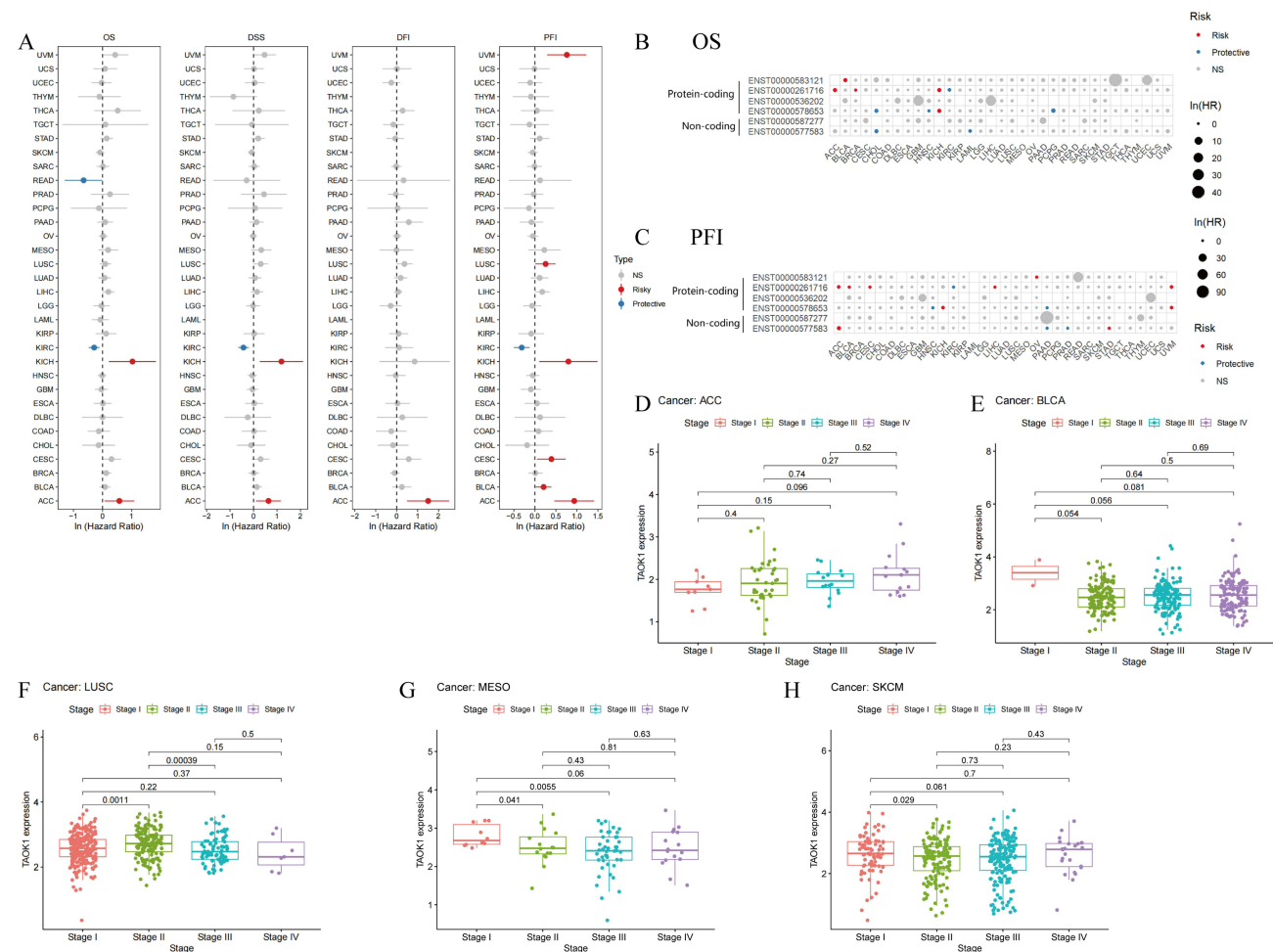


Figure 3 Prognostic analysis of TAOK1. **(A)** The forest plot presents the results of univariate Cox regression analysis of TAOK1, examining OS, DSS, DFI, and PFI. Heatmap illustrates the analysis of OS **(B)** and PFI **(C)** using six TAOK1 transcripts across 33 cancer types from TCGA dataset. The correlation between TAOK1 and clinicopathological stage is explored in multiple tumor types, including ACC **(D)**, BLCA **(E)**, LUSC **(F)**, MESO **(G)**, and SKCM **(H)**. **Abbreviations:** OS, Overall Survival; DSS, Disease-Specific Survival; DFI, Disease-Free Interval; PFI, Progression-Free Interval; NS, Not Significant.

outcomes (Supplement Figure 3A–E). Simultaneously, after conducting survival analysis on TAOK1 transcripts, we found that the TAOK1 coding region is a risk factor in patients' OS, DSS, DFI, and PFI. Moreover, we identified ACC, BLCA, BRCA, and KICH as risk factors in OS analysis (Figure 3B), and ACC, BLCA, CESC, LIHC, OV, and UVM as risk factors in PFI analysis (Figure 3C). Based on both gene and transcript survival analysis, TAOK1 exhibited significant correlation with DFI and DSS in CESC and ACC (Supplement Figure 4A and B). Furthermore, we explored the association between TAOK1 gene expression and tumor stage. Significant correlations were observed in ACC, BLCA, LUSC, MESO, and SKCM (Figure 3D–H).

Additionally, by utilizing the “OncoPredict” software package in combination with the GDSC v2 database, we conducted an analysis of the correlation between the sensitivity of 198 anti-tumor drugs and TAOK1 (refer to Supplement Figure 5A). Our findings reveal a notable inverse correlation between TAOK1 expression and anti-cancer drugs across various tumor types, encompassing OV, THYM, CESC, and READ (Supplement Figure 5B–E). Furthermore, drug sensitivity analysis carried out using the CellMiner database revealed significant results: a positive correlation was identified between TAOK1 expression and the anti-tumor drugs XAV-939 and Irofulven, while a negative correlation was observed between TAOK1 expression and Timazid and Barasertib (Supplement Figure 5F). Our study uncovered a correlation between the expression of TAOK1 and multiple drugs in diverse tumor types, suggesting a distinct association between TAOK1 expression and tumor type. In conclusion, our research underscores the substantial prognostic importance of TAOK1 in a variety of cancer types.

TAOK1 Correlates with Tumor Stemness and Tumor Immunity

To clarify the role of TAOK1 in the tumour immune response, we conducted a comprehensive survey of a range of tumour types. Using the XCELL algorithm, we assessed the correlation between TAOK1 expression levels and infiltration levels of different immune cell subsets in tumours. A negative correlation was found between TAOK1 expression and the majority of immune cells (Figure 4A), including T cells, Macrophage M1, T cell CD4+ Th1 and others. In addition, we found a significant negative correlation between TAOK1 expression and tumour fibroblasts (CAF) (Figure 4B), stromal scores (Figure 4C) and immune microenvironment scores (Figure 4D), while a positive correlation was found with T cell regulatory populations (Tregs) (Figure 4E). Our analysis specifically uncovered a negative correlation between TAOK1 expression and tumor mutational burden (TMB) across multiple tumor types, including USC, THCA, STAD, PCPG, PAAD, LUSC, LIHC, KIRP, KIRC, ESCA, DLBC, CESC, and BRCA. TAOK1 expression was positively correlated with TMB in several types of cancer. (Supplement Figure 6A). In addition, a significant association between TAOK1 expression and microsatellite instability (MSI) status was observed in 11 tumors (Supplement Figure 6B). Specifically, TAOK1 exhibited a positive correlation with MSI in UCEC, READ, LUSC, and CESC, while a negative correlation was observed in THCA, SKCM, PRAD, KIRP, HNSC, DLBC, and BRCA.

Furthermore, our analysis found an association between TAOK1 and immune checkpoints in different tumor types (Figure 4F). Additionally, correlation analysis demonstrated significant associations between TAOK1 expression and several immunomodulatory factors (Supplement Figure 7A), with notable negative correlations observed with CD27, IL23A, and LAG3, and positive correlations with CD80, STAT3, and IL17RA (Supplement Figure 7B–G).

Furthermore, given the importance of stemness-related biomarkers in the field of tumor biology, we delved into the association between DNA stemness (DNAss) and RNA stemness (RNAss) and TAOK1. Our results showed

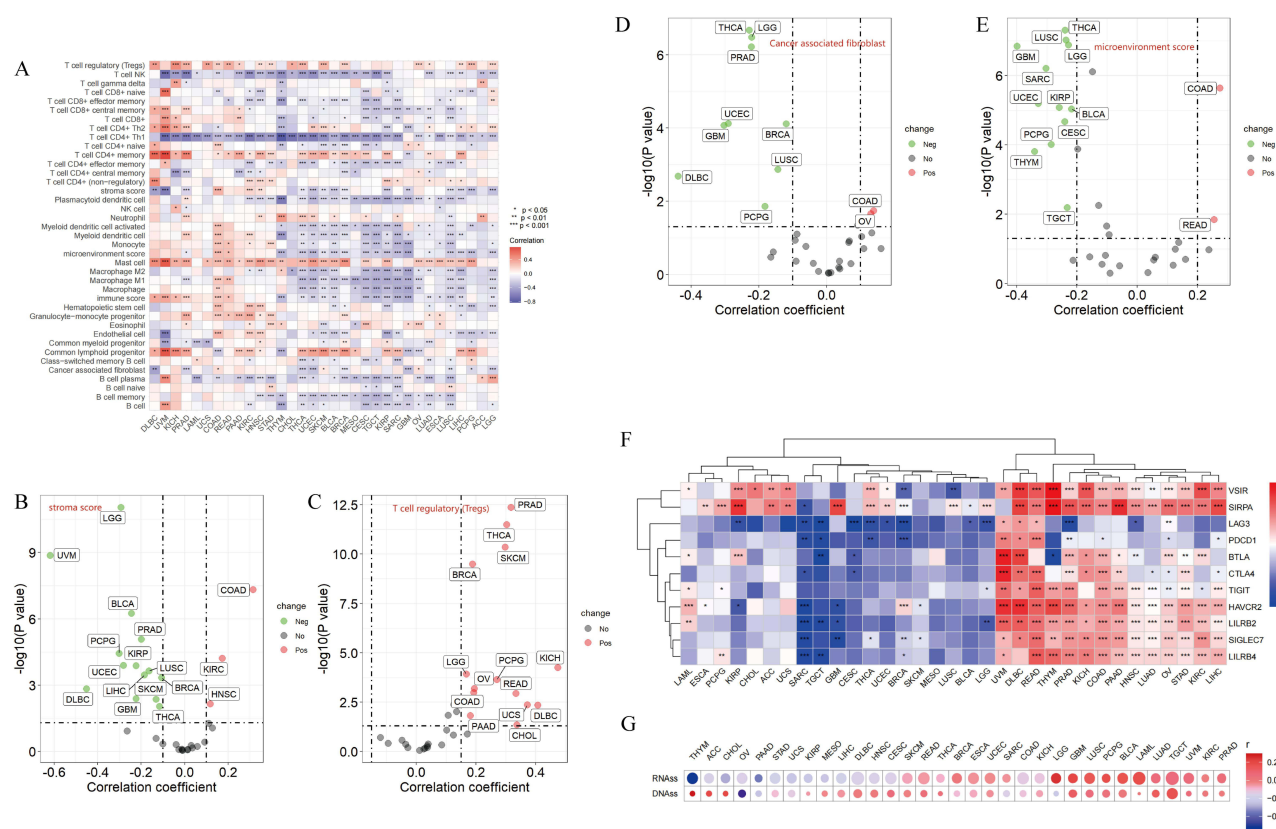


Figure 4 The immune correlation analysis of TAOK1. (A) Heatmaps were generated to visually represent the relationship between TAOK1 and different immune infiltrating cells and quantified using the XCELL algorithm. Color gradients from purple to red denote correlation coefficients. A scatter plot demonstrates Spearman correlation analysis based on the XCELL algorithm, depicting the relationship between TAOK1 expression in tumors and (B) tumor fibroblast infiltration, (C) stromal score, (D) microenvironment score, and (E) regulatory T cell (Tregs) infiltration. (F) Heatmap depicting the correlation between TAOK1 and 11 immune checkpoints. (G) Correlation analysis between TAOK1 and tumor stemness, assessed via DNA and RNA stemness indices. * $P < 0.05$; ** $P < 0.01$; *** $P < 0.001$.

a predominantly positive correlation between TAOK1 expression and stemness score in most tumor types (Figure 4G). Notably, however, in ovarian cancer, TAOK1 was negatively correlated with both RNA stemness (RNAss) and DNA stemness (DNAss). Collectively, our results underscore the significant role of TAOK1 in modulating immune responses across a spectrum of tumor types.

GSEA Functional Enrichment Analysis of TAOK1's Functional Significance

In order to delve deeper into the biological relevance of TAOK1 across various tumor types, an extensive analysis was conducted to examine its participation in Kyoto Encyclopedia of Genes and Genomes (KEGG) pathways and biological processes utilizing the GSEA database (Figure 5A and B). Our KEGG enrichment analysis revealed significant enrichment of pathways pertinent to several cancer types. Notably, these pathways encompassed critical processes such as pathways in cancer, T cell signaling pathway, wnt signaling pathway and focal adhesion (Supplement Figure 8A–E). Furthermore, our GSEA correlation analysis of biological processes unveiled a plethora of associations with TAOK1 (Figure 5B). These included, but were not limited to, the regulation of DNA repair, immune system development (Supplement Figure 8F and G), and viral transcription, among others.

Furthermore, at the gene expression level, we detected significant correlations between TAOK1 and various cell cycle (Supplement Figure 9A), cell adhesion, ferroptosis (Figure 5C), and copper death (Figure 5D) related genes. Notably, cell cycle-related genes such as BCL2, CCNB3, and HSP90AA1 (Supplement Figure 9B–D), as well as cell adhesion genes such as ITGA1 (Supplement Figure 9G), demonstrated positive correlations with TAOK1 across multiple tumors; Conversely, genes like MACF1 and ICAM2 exhibited negative correlations with TAOK1 in the majority of tumors (Supplement Figure 9E and F). Additionally, our analysis revealed associations between TAOK1 and genes involved in ferroptosis, including NCOA4, ACSL4, and TFRC (Supplement Figure 10A–C), as well as cuprotoxicosis-related genes like MTF1, DLAT, and GLS (Supplement Figure 10D–F). Furthermore, correlation analyses highlighted distinct patterns in specific cancer types, notably CESC and OV. In CESC, TAOK1 displayed positive correlations with a range of cell cycle-related genes such as ATRX, RBL2, CCNE2, and CDC6 (Figure 5E, F and Supplement Figure 11A–D), alongside cell adhesion-related genes such as CLASP2, MACF1, ITGAV, and TSC1 (Supplement Figure 11E–H). Similarly, in OV, TAOK1 showed positive associations with cell cycle genes like ATRX, RBL2, BCL2L11, and BAX (Figure 5G, H and Supplement Figure 12A–D), as well as cell adhesion-related genes such as CLASP2, EPB41L1, MACF1, and UTRN (Supplement Figure 12E–H). This discovery aligns with the outcomes of Gene Set Enrichment Analysis (GSEA), offering additional understanding of the molecular interactions involving TAOK1 in various forms of cancer.

Genetic Variation Analysis of TAOK1

Subsequently, in order to more deeply investigate the mechanisms driving the upregulation of TAOK1 expression, we began an extensive analysis of mutations, copy number variations (CNVs) and DNA methylation patterns within the TAOK1 gene. Using the extensive TCGA pan-cancer dataset available through the cBioportal database, we discovered interesting findings. Our research revealed different mutations of TAOK1 in different tumor types, with the most notable mutation rate being observed in endometrial cancer, which reached 4.95% (Figure 6A). Next, we scrutinized the relationship between TAOK1 and CNV in different tumors. Our results showed that in most tumor types (eg BLCA and KIRP), TAOK1 had a high percentage of CNV amplification. On the contrary, in a few tumor types, such as ACC, KICH, and OV, the proportion of TAOK1 deletions was higher (Figure 6B). In addition, a significant positive correlation ($r > 0.2$; $P < 0.05$) was shown between copy number variations of TAOK1 and expression of TAOK1 based on correlation analysis (Supplement Figure 13A), with the four tumor types with the highest correlations being READ ($r = 0.49$); BRCA ($r = 0.46$), LUSC ($r = 0.45$), and UCS ($r = 0.43$) (Supplement Figure 13B–E).

Turning to epigenetic regulation analysis, we explored aberrant methylation patterns within the TAOK1 promoter region, a hallmark of transcriptional dysregulation in cancer. Interestingly, our analysis revealed significant negative correlations between TAOK1 expression and methylation status, particularly in tumor types such as DLBC, ESCA, HNSC, OV, SARC and UCS (Figure 6C). Of particular interest were the methylation sites of cg08491221 and cg15702825, which showed consistent negative correlations across tumor types compared to normal samples

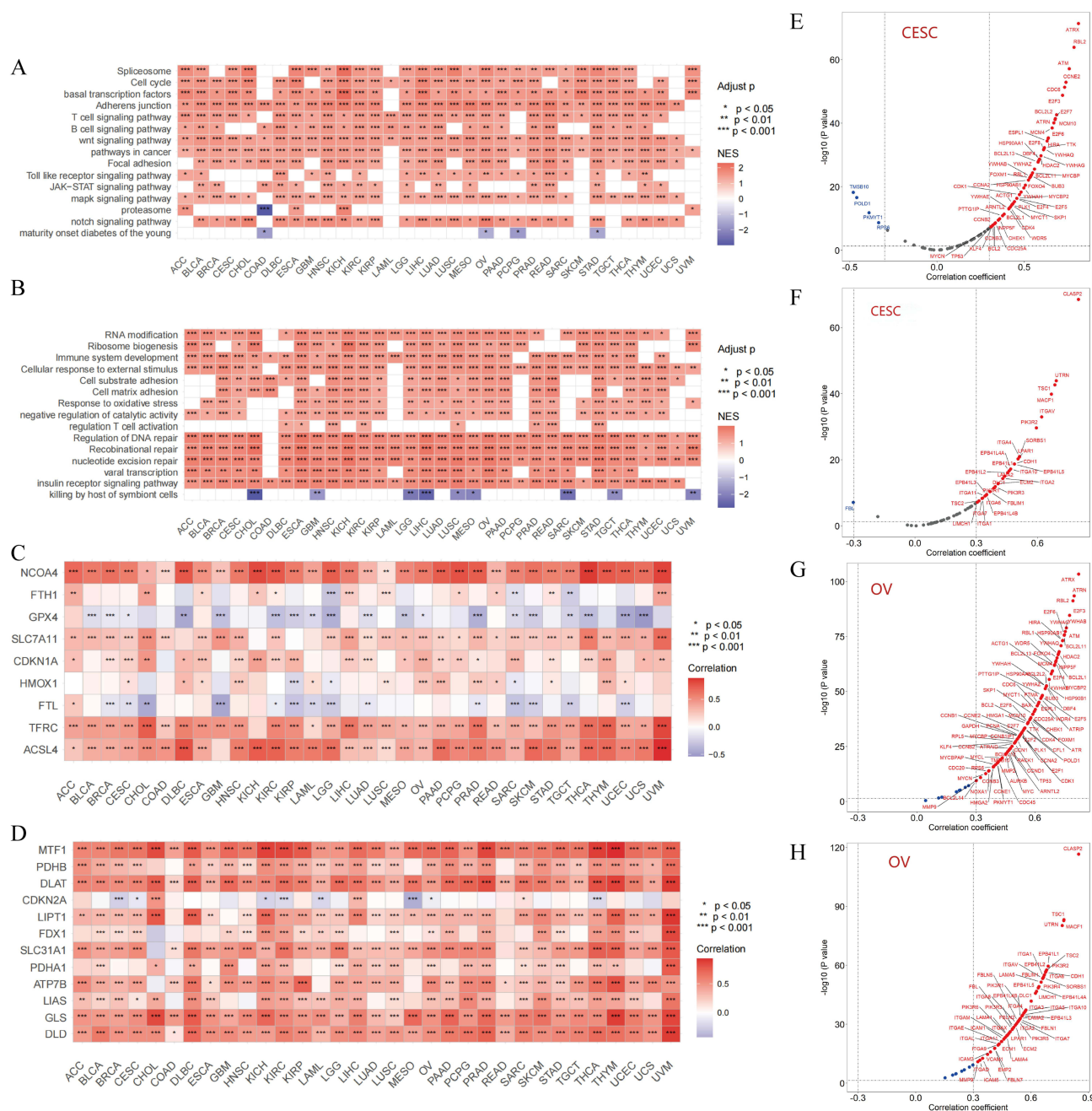


Figure 5 The correlation analysis between TAOK1 pathways and biological processes. **(A)** Heatmaps were generated via GSEA to illustrate the pathways associated with the KEGG and TAOK1. **(B)** Heatmap illustrating biological processes correlated with TAOK1. **(C)** Heatmap presenting an analysis of the association between TAOK1 and genes implicated in ferroptosis. **(D)** Heatmap showcasing a correlation analysis between TAOK1 and genes associated with cuproptosis. Correlation analyses between TAOK1 and cell cycle-related genes **(E)** as well as cell adhesion-related genes **(F)** in CESC. Correlation analyses between TAOK1 and cell cycle-related genes **(G)** along with cell adhesion-related genes **(H)** in OV. Normalized Enrichment Score (NES) is depicted by a color gradient ranging from purple to red; * P < 0.05; ** P < 0.01; *** P < 0.001. **Abbreviations:** GSEA, Genomic Enrichment Analysis; KEGG, Kyoto Encyclopedia of Genes and Genomes.

(Supplement Figure 13F and G). These findings suggest the therapeutic potential of targeting specific methylation sites as a means of regulating TAOK1 expression in cancer therapy.

In conclusion, our comprehensive analysis highlights the multifaceted regulatory environment controlling TAOK1 expression in cancer, suggesting that genomic alterations and epigenetic modifications are key determinants of its dysregulated expression in a wide range of malignancies.

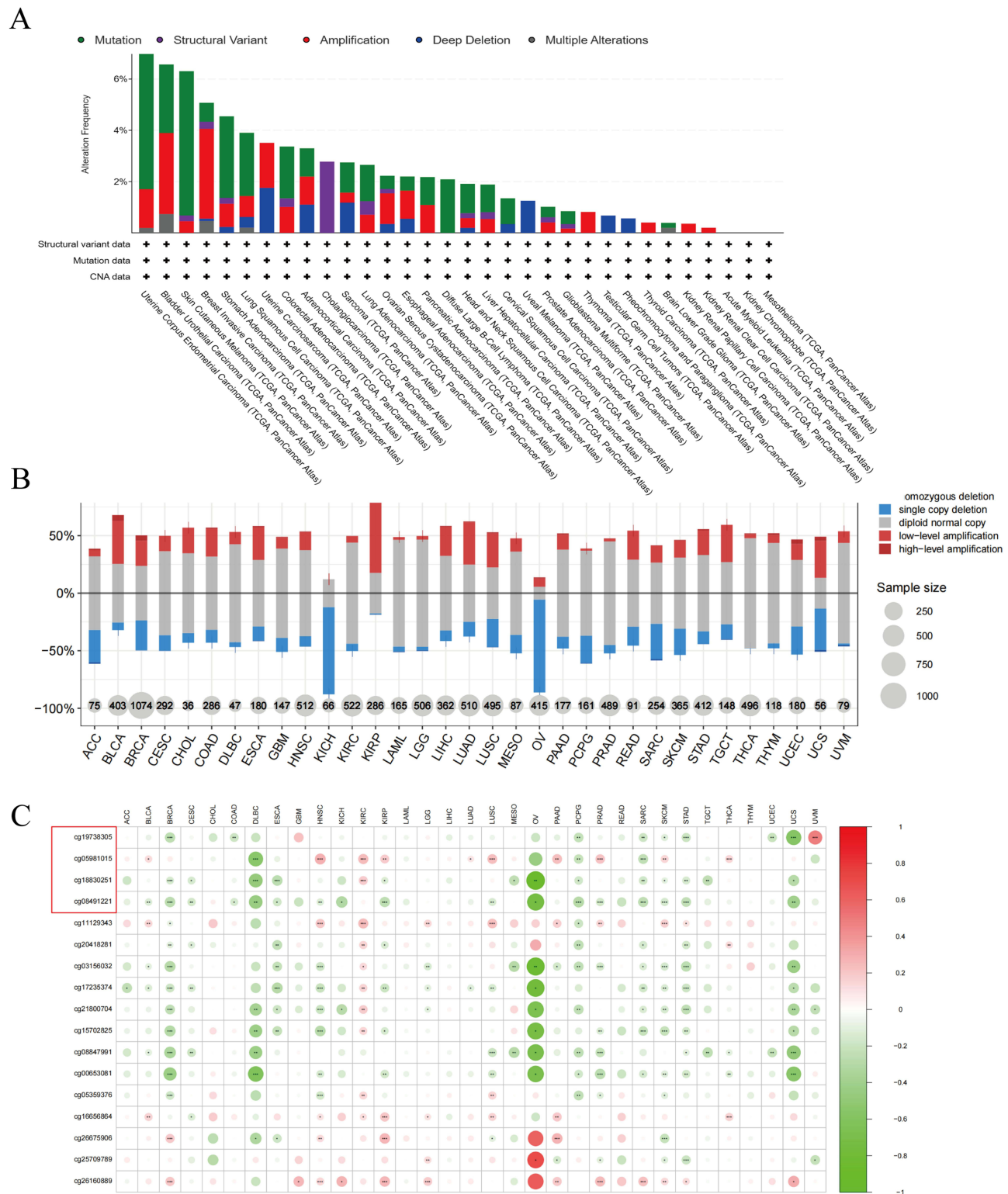


Figure 6 Mutational analysis of DNA copy number variation and DNA methylation in TAOK1. **(A)** Analysis of TAOK1 mutation frequencies in tumors utilizing data from the TCGA database. **(B)** Investigation of DNA copy number variation in TAOK1. **(C)** Examination of methylation mutations in TAOK1, with the red box indicating the promoter region ID of TAOK1. * $P < 0.05$; ** $P < 0.01$; *** $P < 0.001$.

TAOK1 Regulates Proliferation in SiHa and A2780 Cells

To further investigate the biological significance of TAOK1 in human cervical squamous carcinoma (SiHa) and human ovarian cancer (A2780) cell lines, a series of experiments were performed. Small interfering RNA (siRNA) targeting TAOK1

was transfected into these two cell lines and the knockdown efficiency was verified by Western blotting and RT-qPCR. The results showed that Si-1, Si-2 and Si-3 siRNA sequences effectively inhibited TAOK1 expression (Figure 7A and B).

Subsequently, cell proliferation was assessed using the Cell Counting Kit-8 (CCK-8) assay. The results showed that inhibition of TAOK1 significantly suppressed the proliferation of SiHa cells, while the effect on the proliferation of A2780 cells was insignificant. Notably, the inhibitory effect of Si-3 on A2780 cells was minimal (Figure 7C). We further examined the cell cycle of both cell lines by flow cytometry analysis using propidium iodide (PI) staining to further explore the effects on the cell cycle (Figure 7D and E). It was found that inhibition of TAOK1 resulted in a significant shortening of S phase and lengthening of G2 phase in SiHa cells. In contrast, no significant changes in cell cycle were observed in A2780 cells, which prompted us to focus our subsequent studies on the SiHa cell line.

To further explore the regulatory role of TAOK1, we generated SiHa cells stably overexpressing TAOK1 by lentiviral transfection and confirmed the increase in TAOK1 mRNA expression (Figure 7F). We assessed the proliferation of TAOK1-overexpressing SiHa cells by CCK-8 assay (Figure 7G) and analysed cell cycle progression by flow cytometry (Figure 7H) and found that TAOK1 overexpression markedly promoted S-phase growth.

Additionally, we collected eight paired cervical cancer tumor tissues and adjacent non-tumorous tissues for immunohistochemical (IHC) analysis and quantitatively assessed TAOK1 expression using ImageJ software (Figure 7I). The results revealed that TAOK1 expression was significantly higher in cervical cancer tissues compared to adjacent non-tumorous tissues. To determine whether our in vitro findings were consistent with in vivo models, we established xenografts in nude mice by subcutaneously transplanting SiHa cells transfected with TAOK1 overexpression (TAOK1-OE) or Vector controls. One week after transplantation, 100% tumor formation was observed, and tumors were excised. The tumor volume in the TAOK1-OE group (n=5) was significantly larger than that in the Vector group (n=5) (Figure 7J), demonstrating that TAOK1 overexpression promotes tumor proliferation. In conclusion, our findings indicate that TAOK1 plays a critical role in promoting the proliferation of cervical cancer cells.

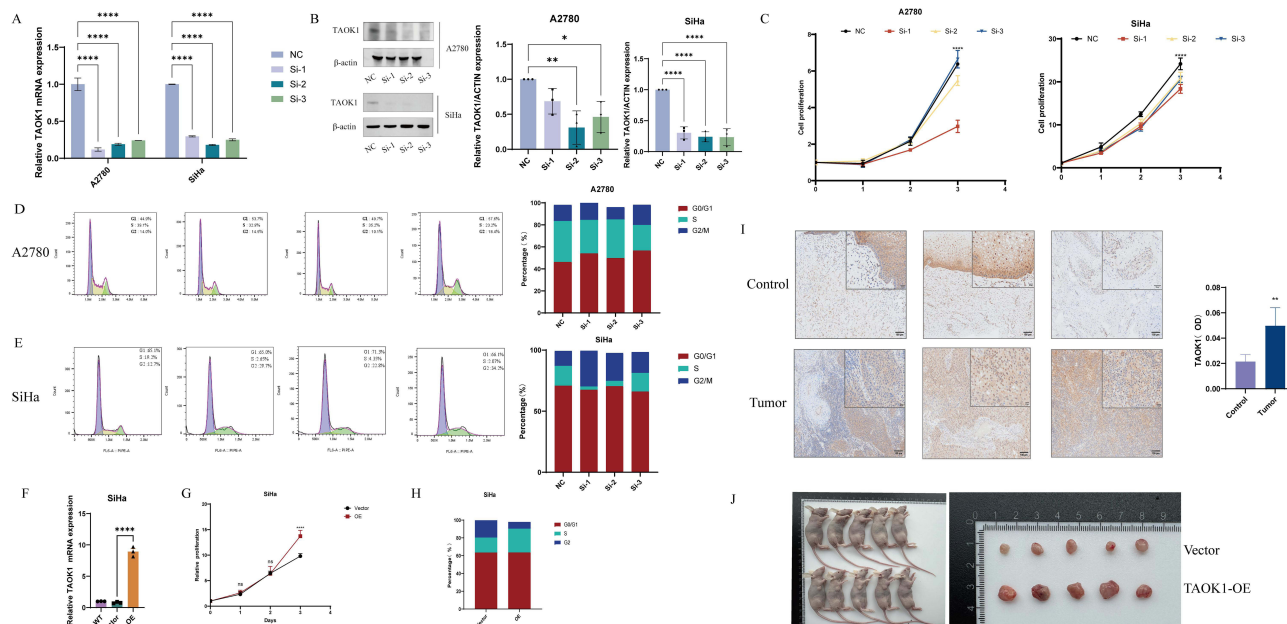


Figure 7 The impact of TAOK1 on the proliferation of A2780 and SiHa cell lines. (A and B) Validation of mRNA and protein expression levels of TAOK1 siRNA in A2780 and SiHa cells by RT-qPCR and Western Blot. (C) Proliferation levels of A2780 and SiHa cells were detected at 24 h, 48 h and 72 h after TAOK1 inhibition using Cell Counting Kit-8 (CCK-8) assay. (D and E) The effects of TAOK1 inhibition on the cell cycle of A2780 and SiHa cells were analysed using flow cytometry. (F) Overexpression levels of TAOK1 in SiHa cell lines were verified using RT-qPCR. (G) Proliferation level of SiHa cells after TAOK1 overexpression was assessed by CCK-8. (H) The effect of TAOK1 overexpression on SiHa cell cycle was analysed by flow cytometry. (I) The expression levels of TAOK1 in tumour tissues and their adjacent normal tissues of cervical cancer patients were detected by immunohistochemistry (IHC), and representative images are shown. Control group: adjacent normal tissues; tumour group: cervical cancer tissues. (J) BALB/c nude mice (5 mice per group) were subcutaneously inoculated with SiHa cells stably expressing Vector and TAOK1. ns, not significant; * $p < 0.05$ indicates statistically significant difference; ** $P < 0.01$; *** $P < 0.001$; **** $P < 0.0001$.

Correlation Analysis of TAOK1 With the Transcription Factor EP300

To comprehensively investigate TAOK1's upstream regulatory mechanisms, we employed three transcription factor prediction network tools alongside the OV and CESC datasets to identify potential transcription factors involved in its regulation. Based on the results of correlation analysis, we identified ten transcription factors that were significantly correlated with TAOK1 expression (Figure 8A). Further analysis of the OV and CESC datasets revealed a significant correlation between TAOK1 and EP300 (Supplement Figure 14A).

To validate these findings, we measured the mRNA expression levels of the ten identified transcription factors using RT-qPCR after transfecting SiHa and A2780 cell lines with small interfering RNA (siRNA) targeting TAOK1 (Figure 8B and C). The results demonstrated a marked reduction in the expression of EP300, which corroborated the results from the correlation analysis. Additionally, we performed correlation analyses of TAOK1 and EP300 using the TCGA and CCLE databases. The analyses revealed a strong correlation between these two genes, as shown in the TCGA database (Figure 8D and F) and the CCLE database (Figure 8E). The datasets exhibiting the highest correlations in the TCGA cohort were THYM ($r = 0.92$), PRAD ($r = 0.92$), and CHOL ($r = 0.91$) (Supplement Figure 14B–D). In conclusion, it was shown that there is a significant correlation between TAOK1 and the transcription factor EP300, demonstrating a clear regulatory relationship between the two.

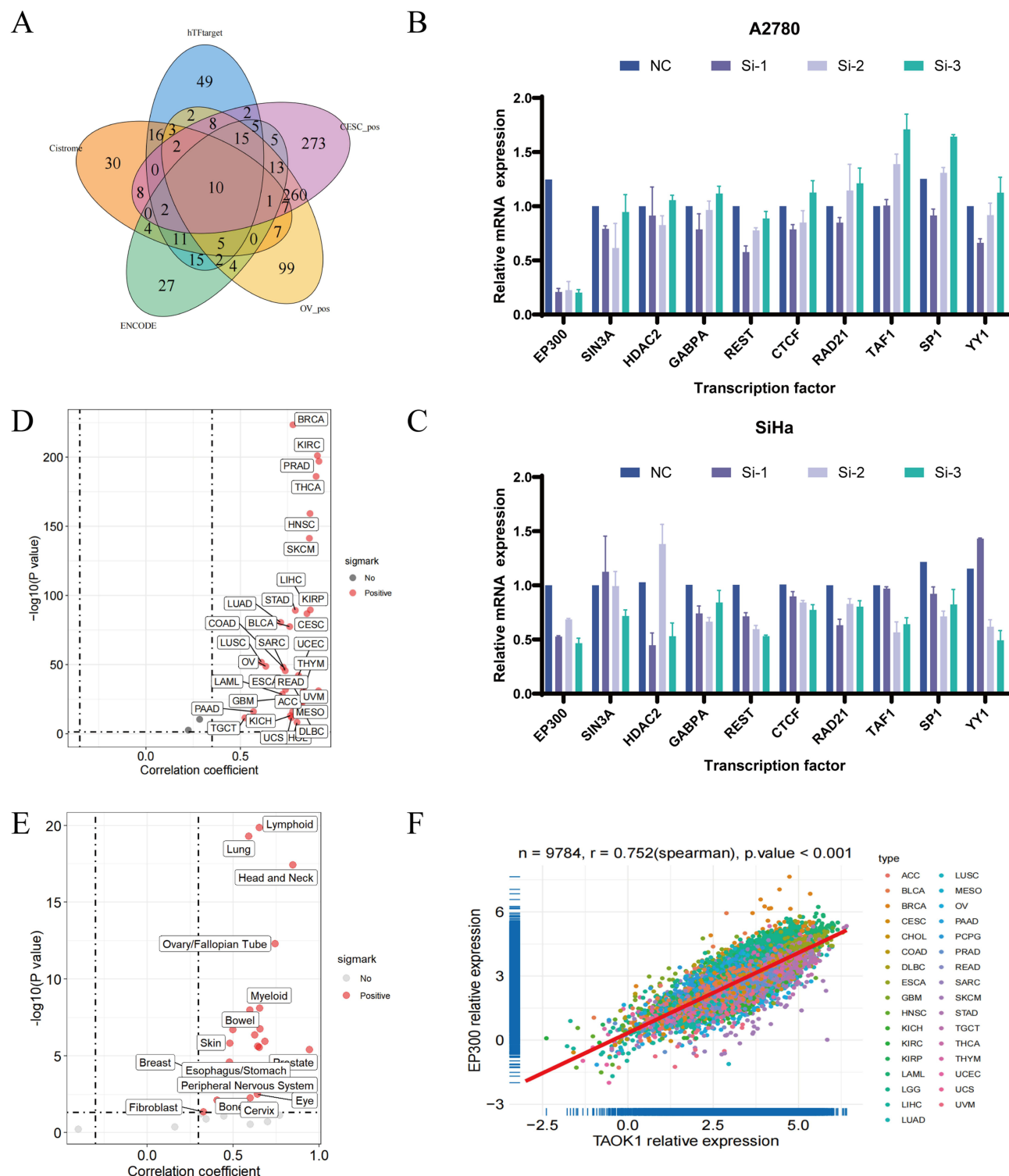
Discussion

The Ste20 kinase family is recognized for its involvement in kinase signaling pathways that govern signal transduction.¹⁰ Increased expression of TAOK1 has been associated with various forms of tumors, with its aberrant expression playing a role in the onset and advancement of multiple malignancies.²² As a result, there is a rising interest in investigating TAOK1 kinase inhibitors as promising therapeutic targets for these cancers. This study uses a series of bioinformatics studies combined with in vitro experiments to comprehensively study the function and regulatory mechanism of TAOK1 in different tumors. Previous studies have indicated elevated TAOK1 expression across numerous tumor types, including ovarian,¹⁵ colorectal,¹⁴ esophageal squamous cell,¹² non-small cell lung¹³ and liver cancers.²³ Our pan-cancer analysis based on the TCGA database corroborates these findings, revealing significant differences in TAOK1 expression across different tumor types, with a predominant upward trend observed in most cases. Moreover, patients with higher TAOK1 expression levels exhibited poorer prognoses.

Furthermore, our analysis identified a clear correlation between TAOK1 and tumor status at the transcript level, suggesting potential transcriptional regulation of TAOK1. We evaluated the relationship between patient survival and the TAOK1 gene, focusing on indicators such as OS, DSS, DFI, PFI. Notably, the relationship was most pronounced in patients with ACC. Furthermore, our examination of drug sensitivity demonstrated a notable inverse relationship between TAOK1 expression and the effectiveness of various anti-tumor medications, suggesting the possibility of targeted treatment via TAOK1 suppression, in alignment with prior research. Notably, in non-small cell lung cancer (NSCLC), TAOK1 emerged as a key determinant of sensitivity to BET inhibitors (BETi).²⁴ These results collectively underscore the importance of TAOK1 in tumor biology and its potential as a therapeutic target in cancer treatment.

Immunotherapy has emerged as a promising strategy to modulate the tumor microenvironment and inhibit the progression of both localized and metastatic tumors, with its clinical potential becoming increasingly evident.²⁵ Notably, contemporary oncology treatments often focus on immune checkpoint blockade to reshape the immune microenvironment.²⁶ Interestingly, our findings reveal a negative correlation between TAOK1 expression and various immune cell populations, including cancer-associated fibroblasts (CAF) and CD8⁺ T cells, as well as a negative association between the immune microenvironment score and extracellular matrix components. The significant negative correlation between TAOK1 and most of the immune cells proves that we should target TAOK1 inhibition to enhance the ability of immune cells to attack tumours in future therapy. Additionally, analysis of immune checkpoint relationships demonstrated a negative correlation between TAOK1 expression and most immune checkpoints. These findings suggest that targeting TAOK1 inhibition may be a viable strategy for controlling tumor growth in future cancer therapies.

Previous studies have established a negative correlation between immune profiling and stemness, with higher DNA stemness (DNAss) and RNA stemness (RNAss) levels associated with poor prognosis, increased tumor mutational



burden, and heightened infiltration of immune and stromal cells.²⁷ In our study, we identified a significant correlation between TAOK1 expression and tumor stemness scores, with particularly high stemness scores observed in cervical squamous cell carcinoma (CESC). These results underscore the intricate interplay between TAOK1 expression, immune characteristics, and tumor stemness, further highlighting its potential as a therapeutic target in cancer treatment.

Furthermore, genomic heterogeneity analysis revealed a significant correlation between TAOK1 expression and tumor mutational burden (TMB) as well as microsatellite instability (MSI). This aligns with prior research linking TAOK1 to chromosomal structural instability, suggesting that TAOK1 may serve as a critical hub for genetic alterations across different tumor types.²⁸ Notably, TAOK1 mutations were observed in the form of gene truncations, nonsense mutations, and missense mutations, with missense mutations in the kinase domain previously shown to result in loss of kinase activity and neurodevelopmental deficits.²⁹ Our study further confirmed the prevalence of TAOK1 mutations in various cancers, with the highest mutation rate observed in endometrial cancer. Aberrant alterations in DNA methylation, including hypermethylation and hypomethylation, are strongly associated with tumorigenesis, and their ability to act as a marker of tumor-associated genomic instability.³⁰ Studies have demonstrated a correlation between gene copy number variations, DNA methylation, and chromosomal instability. In the present study, copy number alterations and aberrant DNA methylation of TAOK1 were identified in the majority of tumors. These findings suggest that the oncogenic role of TAOK1 may be influenced by its mutational landscape and highlight its potential as a target for personalized therapeutic strategies based on specific genetic alterations.

In our biological analysis, we utilized Gene Set Enrichment Analysis (GSEA) to assess the correlation between TAOK1 and various cancer-related signaling pathways and biological processes. Previous studies have demonstrated that TAOK1 plays a crucial role in kinase signaling and cell mitosis.^{9,10} These processes have a significant impact on tumorigenesis and progression. Additionally, TAOK1 has been shown to regulate the Hippo signaling pathway, where its depletion disrupts the expression of HAP/TAZ, a key effector of the pathway, thereby impairing its activation and influencing tumor progression.³¹ In recent years, mounting evidence has underscored the pivotal role of metabolic cell death in cancer therapy, as underscored by investigations into phenomena such as ferroptosis and cuproptosis.²¹ These forms of cell death offer promising avenues for therapeutic intervention. TAOK1 has been identified as an upstream regulator of the MAPK and JNK signaling pathways, both of which are involved in reactive oxygen species (ROS) generation and lipid peroxidation, key mechanisms in ferroptosis. Additionally, previous research has indicated that upregulation of FDX1 and activation of the MAPK signaling pathway can regulate cuproptosis, thereby inhibiting the growth of hepatocellular carcinoma. Based on these findings, we analyzed the correlation between TAOK1 and two key cell death-related genes and observed a significant association. These results provide strong evidence for the potential role of TAOK1 as a therapeutic target and lay the foundation for the development of novel cancer treatment strategies. Notably, TAOK1 exhibited a significant positive correlation with pathways involved in cell cycle regulation, T-cell signaling, Wnt signaling, and cell-substrate adhesion, particularly in cervical squamous cell carcinoma (CESC) and ovarian cancer (OV). These pathways are known to regulate key tumorigenic processes, including proliferation, migration and invasion.^{32,33} To further elucidate the specific role of TAOK1 in cervical and ovarian cancers, we selected SiHa and A2780 cell lines for experimental validation. Our results showed that knockdown of TAOK1 significantly inhibited the proliferation of both cell types, with a more pronounced effect observed in the SiHa cell line. Subsequently, we constructed a plasmid overexpressing TAOK1 and transfected the SiHa cell line, and successfully constructed a TAOK1 overexpression stable transplants. Both in vitro and in vivo experiments demonstrate that TAOK1 overexpression significantly enhances tumor growth, providing further theoretical support for TAOK1 as a potential therapeutic target for cervical cancer. Therefore, targeting TAOK1 through gene silencing or small molecule inhibitors can be used as an effective strategy to inhibit cervical cancer. Despite these findings, our study still has some limitations. Although we performed in vitro and in vivo validation using cervical cancer cells, no similar experiments were performed on ovarian cancer. Given the long time required for this study and the complexity of constructing ovarian cancer overexpressing cell lines, future studies will focus on validating these findings in ovarian cancer and other tumor types. Additional in vitro and in vivo studies will also be conducted to confirm the role of TAOK1 as a tumor prognostic and therapeutic target.

Notably, the transcription factor EP300 is thought to regulate the expression level of TAOK1, and additionally in cervical cancer EP300 has been shown to be associated with the promotion of cervical cancer proliferation.³⁴ Previous studies have highlighted the different roles of EP300 in various cancers: in colon cancer, its regulation is associated with protein degradation;³⁵ in non-small cell lung cancer, mutations in the EP300 gene have been shown to accelerate tumor progression;³⁶ and in prostate cancer, therapeutic strategies have focused on attenuating the inhibitory effects of EP300 in order to modulate transcription factor signaling.³⁷ In light of these findings, targeting EP300 to regulate TAOK1 expression may be a promising approach to influence tumor progression in future studies.

Conclusions

In this study, we showed that TAOK1 was closely associated with poor prognosis in cervical squamous cell carcinoma and ovarian cancer, and its upregulation in most tumours was regulated by DNA copy number, methylation status and the transcription factor EP300. TAOK1 was significantly negatively correlated with immune-infiltrating cells and immune checkpoints, and the effect of TAOK1 inhibition on the proliferation of SiHa and A2780 cells was verified by in vitro experiments effects, especially in SiHa cells. This result was further verified by in vivo animal experiments, indicating that TAOK1 could significantly promote the proliferation of cervical cancer. Despite the limitations of this study, such as the lack of ex vivo and in vivo studies of TAOK1 in other tumour types, TAOK1, as a promising prognostic biomarker and immunotherapeutic target, provides new insights into clinical drug development and therapeutic strategies for cervical cancer.

Ethical Approval and Informed Consent

This study complies with the Declaration of Helsinki. The study was ethically approved by the Ethics Committee of the Affiliated Hospital of Nanjing University of Chinese Medicine (Ethics Approval No. 2021NL-025-03). All animal experiments were approved by the Ethics Committee of the Affiliated Hospital of Nanjing University of Traditional Chinese Medicine (Ethics Approval No.2024DW-101-01).

Acknowledgments

This research was funded by the National Natural Science Foundation of China (Grant No. 82074478), the Chinese Clinical Medicine Innovation Center of Obstetrics, Gynecology, and Reproduction in Jiangsu Province (Grant No. ZX202102).

Author Contributions

All authors made significant contributions to the conception and design of the study, data collection, analysis or interpretation. They actively participated in drafting the manuscript, revising and reviewing it, agreed to submit it to the journal, approved the version to be published, and took responsibility for all aspects of the work.

Disclosure

The authors declare no competing interests in this work.

References

1. Siegel RL, Giaquinto AN, Jemal A. Cancer statistics, 2024. *CA Cancer J Clin.* **2024**;74(1):12–49. doi:10.3322/caac.21820
2. Lu Z, Chen Y, Liu D, et al. The landscape of cancer research and cancer care in China. *Nat Med.* **2023**;29(12):3022–3032. doi:10.1038/s41591-023-02655-3
3. Ferrari F, Giannini A. Approaches to prevention of gynecological malignancies. *BMC Women's Health.* **2024**;24(1):254. doi:10.1186/s12905-024-03100-4
4. Qi L, Li G, Li P, et al. Twenty years of Gendicine® rAd-p53 cancer gene therapy: the first-in-class human cancer gene therapy in the era of personalized oncology. *Genes Dis.* **2024**;11(4):101155. doi:10.1016/j.gendis.2023.101155
5. Zi M, Maqsood A, Prehar S, et al. The mammalian Ste20-like kinase 2 (Mst2) modulates stress-induced cardiac hypertrophy. *J Biol Chem.* **2014**;289(35):24275–24288. doi:10.1074/jbc.M114.562405
6. Getu AA, Zhou M, Cheng SY, Tan M. The mammalian Sterile 20-like kinase 4 (MST4) signaling in tumor progression: implications for therapy. *Cancer Lett.* **2023**;563:216183. doi:10.1016/j.canlet.2023.216183

7. Xiong W, Matheson CJ, Xu M, et al. Structure-based screen identification of a Mammalian Ste20-like kinase 4 (MST4) inhibitor with therapeutic potential for pituitary tumors. *Mol Cancer Ther.* **2016**;15(3):412–420. doi:10.1158/1535-7163.MCT-15-0703
8. Miller CJ, Lou HJ, Simpson C, et al. Comprehensive profiling of the STE20 kinase family defines features essential for selective substrate targeting and signaling output. *PLoS Biol.* **2019**;17(3):e2006540. doi:10.1371/journal.pbio.2006540
9. Koo CY, Giacomini C, Reyes-Corral M, et al. Targeting TAO kinases using a new inhibitor compound delays mitosis and induces mitotic cell death in centrosome amplified breast cancer cells. *Mol Cancer Ther.* **2017**;16(11):2410–2421. doi:10.1158/1535-7163.MCT-17-0077
10. Chao MW, Lin TE, HuangFu WC, et al. Identification of a dual TAOK1 and MAP4K5 inhibitor using a structure-based virtual screening approach. *J Enzyme Inhib Med Chem.* **2021**;36(1):98–108. doi:10.1080/14756366.2020.1843452
11. Schulte I, Batty EM, Pole JC, et al. Structural analysis of the genome of breast cancer cell line ZR-75-30 identifies twelve expressed fusion genes. *Bmc Genomics.* **2012**;13(1):719. doi:10.1186/1471-2164-13-719
12. Song M, Qu Y, Jia H, et al. Targeting TAOK1 with resveratrol inhibits esophageal squamous cell carcinoma growth in vitro and in vivo. *Mol, Carcinog.* **2024**;63(5):991–1008. doi:10.1002/mc.23703
13. Chen L. TAOK1 promotes proliferation and invasion of non-small-cell lung cancer cells by inhibition of WWC1. *Comput Math Methods Med.* **2022**;2022:1–9. doi:10.1155/2022/3157448
14. Capra M, Nuciforo PG, Confalonieri S, et al. Frequent alterations in the expression of serine/threonine kinases in human cancers. *Cancer Res.* **2006**;66(16):8147–8154. doi:10.1158/0008-5472.CAN-05-3489
15. Beg A, Parveen R, Fouad H, Yahia ME, Hassanein AS. Identification of driver genes and miRNAs in ovarian cancer through an integrated in-silico approach. *Biology.* **2023**;12(2):192. doi:10.3390/biology12020192
16. Liskovych M, Goncharov NV, Petrov N, et al. A novel assay to screen siRNA libraries identifies protein kinases required for chromosome transmission. *Genome Res.* **2019**;29(10):1719–1732. doi:10.1101/gr.254276.119
17. Li F, Yoshizawa JM, Kim KM, et al. Discovery and validation of salivary extracellular RNA biomarkers for noninvasive detection of gastric cancer. *Clin Chem.* **2018**;64(10):1513–1521. doi:10.1373/clinchem.2018.290569
18. Esteban-Fabró R, Willoughby CE, Piqué-Gili M, et al. Cabozantinib enhances anti-PD1 activity and elicits a neutrophil-based immune response in hepatocellular carcinoma. *Clin Cancer Res.* **2022**;28(11):2449–2460. doi:10.1158/1078-0432.CCR-21-2517
19. Vathipadikeal V, Wang V, Wei W, et al. Creation of a human secretome: a novel composite library of human secreted proteins: validation using ovarian cancer gene expression data and a virtual secretome array. *Clin Cancer Res.* **2015**;21(21):4960–4969. doi:10.1158/1078-0432.CCR-14-3173
20. Feng L, Wang J, Cao B, et al. Gene expression profiling in human lung development: an abundant resource for lung adenocarcinoma prognosis. *PLoS One.* **2014**;9(8):e105639. doi:10.1371/journal.pone.0105639
21. Mao C, Wang M, Zhuang L, Gan B. Metabolic cell death in cancer: ferroptosis, cuproptosis, disulfidptosis, and beyond. *Protein Cell.* **2024**;pwae003. doi:10.1093/procel/pwae003
22. Bai Z, Yao Q, Sun Z, Xu F, Zhou J. Prognostic value of mRNA expression of MAP4K family in acute myeloid leukemia. *Technol Cancer Res Treat.* **2019**;18:153303381987392. doi:10.1177/1533033819873927
23. Xia Y, Andersson E, Anand SK, et al. Silencing of STE20-type kinase TAOK1 confers protection against hepatocellular lipotoxicity through metabolic rewiring. *Hepatol Commun.* **2023**;7(4):e0037. doi:10.1097/H9.0000000000000037
24. Gobbi G, Donati B, Do Valle IF, et al. The Hippo pathway modulates resistance to BET proteins inhibitors in lung cancer cells. *Oncogene.* **2019**;38(42):6801–6817. doi:10.1038/s41388-019-0924-1
25. Luke JJ, Davar D, Andtbacka RH, et al. Society for Immunotherapy of Cancer (SITC) recommendations on intratumoral immunotherapy clinical trials (IICT): from premalignant to metastatic disease. *J ImmunoTher Cancer.* **2024**;12(4):e008378. doi:10.1136/jitc-2023-008378
26. Topalian SL, Forde PM, Emens LA, Yarchoan M, Smith KN, Pardoll DM. Neoadjuvant immune checkpoint blockade: a window of opportunity to advance cancer immunotherapy. *Cancer Cell.* **2023**;41(9):1551–1566. doi:10.1016/j.ccell.2023.07.011
27. Romano S, Tufano M, D'Arrigo P, Vigorito V, Russo S, Romano MF. Cell stemness, epithelial-to-mesenchymal transition, and immunoevasion: intertwined aspects in cancer metastasis. *Semin Cancer Biol.* **2020**;60:181–190. doi:10.1016/j.semcancer.2019.08.015
28. Kouprina N, Liskovych M, Petrov N, Larionov V. Human artificial chromosome (HAC) for measuring chromosome instability (CIN) and identification of genes required for proper chromosome transmission. *Exp Cell Res.* **2020**;387(2). doi:10.1016/j.yexcr.2019.111805
29. Tao Z, Wang S, Wu C, et al. The repertoire of copy number alteration signatures in human cancer. *Brief Bioinform.* **2023**;24(2):bbad053. doi:10.1093/bib/bbad053
30. Di Micco R, Krizhanovsky V, Baker D, d'Adda Di Fagagna F. Cellular senescence in ageing: from mechanisms to therapeutic opportunities. *Nat Rev Mol Cell Biol.* **2021**;22(2):75–95. doi:10.1038/s41580-020-00314-w
31. Poon CLC, Lin JI, Zhang X, Harvey KF. The sterile 20-like kinase Tao-1 controls tissue growth by regulating the Salvador-Warts-Hippo pathway. *Dev Cell.* **2011**;21(5):896–906. doi:10.1016/j.devcel.2011.09.012
32. Wen P, Jiang D, Qu F, et al. PFDN5 plays a dual role in breast cancer and regulates tumor immune microenvironment: insights from integrated bioinformatics analysis and experimental validation. *Gene.* **2025**;933:149000. doi:10.1016/j.gene.2024.149000
33. Gomathinayagam S, Srinivasan R, Gomathi A, et al. Oral administration of carotenoid-rich dunaliella salina powder inhibits colon carcinogenesis via modulation of Wnt/ β -catenin signaling cascades in a rat model. *Appl Biochem Biotechnol.* **2025**;197(1):159–178. doi:10.1007/s12010-024-05024-z
34. Yu J, Gui X, Zou Y, et al. A proteogenomic analysis of cervical cancer reveals therapeutic and biological insights. *Nat Commun.* **2024**;15(1):10114. doi:10.1038/s41467-024-53830-0
35. Wu SY, Chu CA, Lan SH, Liu HS. Degradative autophagy regulates the homeostasis of miRNAs to control cancer development. *Autophagy.* **2024**;1–3. doi:10.1080/15548627.2024.2312035
36. Kim KB, Kabra A, Kim DW, et al. KIX domain determines a selective tumor-promoting role for EP300 and its vulnerability in small cell lung cancer. *Sci Adv.* **2022**;8(7):eabl4618. doi:10.1126/sciadv.abl4618
37. Huttunen J, Aaltonen N, Helminen L, Rilla K, Paakinaho V. EP300/CREBBP acetyltransferase inhibition limits steroid receptor and FOXA1 signaling in prostate cancer cells. *Cell Mol Life Sci.* **2024**;81(1):160. doi:10.1007/s00018-024-05209-z

OncoTargets and Therapy

Publish your work in this journal

OncoTargets and Therapy is an international, peer-reviewed, open access journal focusing on the pathological basis of all cancers, potential targets for therapy and treatment protocols employed to improve the management of cancer patients. The journal also focuses on the impact of management programs and new therapeutic agents and protocols on patient perspectives such as quality of life, adherence and satisfaction. The manuscript management system is completely online and includes a very quick and fair peer-review system, which is all easy to use. Visit <http://www.dovepress.com/testimonials.php> to read real quotes from published authors.

Submit your manuscript here: <https://www.dovepress.com/oncotargets-and-therapy-journal>

Dovepress
Taylor & Francis Group